*Pedosphere* **31**(5): 725–735, 2021
doi:10.1016/S1002-0160(21)60022-X
ISSN 1002-0160/CN 32-1315/P

Published by Elsevier B.V. and Science Press

PEDOSPHERE

www.elsevier.com/locate/pedosphere

# Integrated analysis reveals an association between the rhizosphere microbiome and root rot of arecanut palm

Hong LI[1], Xiang MA[1], Yanqiong TANG[1], Chengliang YAN[1], Xinwen HU[1], Xi HUANG[1], Min LIN[2] and Zhu LIU[1,*]

[1]*Key Laboratory of Tropical Biological Resources of Ministry of Education, School of Life and Pharmaceutical Sciences, Hainan University, Haikou 570228 (China)*
[2]*Biotechnology Research Institute, Chinese Academy of Agricultural Sciences, Beijing 100081 (China)*

(Received September 19, 2019; revised January 21, 2020)

## ABSTRACT

The rhizosphere microbial community is crucial to plant health. Many studies have explored the association between the rhizosphere microbiome and plant disease. However, few studies have focused on root rot in arecanut palm, a disease causing devastating effects and thus resulting in economic losses that considerably affect the development of the arecanut industry. Here, rhizosphere samples were collected from both healthy arecanut palm plants and root-rotted arecanut palm plants, and the microbial communities were analyzed using high-throughput sequencing. The root-rotted samples exhibited distinct microbial community richness, diversity, and composition compared with the healthy samples, which was associated with pH according to the Mantel test. Identified potential plant pathogens, including Proteobacteria, Bacteroidetes, Chytridiomycota, and Mortierellomycota, were significantly enriched in the root-rotted samples. In contrast, potentially beneficial plant microbes, such as Acidobacteria and Gemmatimonadetes, were significantly depleted in the root-rotted samples. Co-occurrence networks were constructed to further identify microbial relationships in the root-rotted samples. These findings revealed ecological imbalance among beneficial bacteria in the root-rotted samples. The present study therefore provides an integrated view of the association between the microbial community and root rot in arecanut palm.

*Key Words*: microbial community, co-occurrence network, ecological imbalance, soil physicochemical characteristics, high-throughput sequencing

**Citation**: Li H, Ma X, Tang Y Q, Yan C L, Hu X W, Huang X, Lin M, Liu Z. 2021. Integrated analysis reveals an association between the rhizosphere microbiome and root rot of arecanut palm. *Pedosphere*. **31**(5): 725–735.

## INTRODUCTION

The arecanut palm (*Areca catechu* L.) is cultivated extensively in the tropical Pacific, Asia, and parts of east Africa. In China, there are more 160 000 ha of arecanut palm plantations, most of which are found in Hainan Province. Arecanut has important medicinal value and is regarded as one of four southern medicines in China (Peng *et al*., 2015). However, various field diseases decrease the yield of arecanut and cause serious economic losses to farmers. One disease of particular concern is root rot, which has hindered the development of the arecanut industry in Hainan Province. Many preventive strategies, including fumigation and fungicides, have been applied to control the disease; however, these strategies generally result in environmental pollution.

Soil microbes, such as plant growth-promoting rhizobacteria and mycorrhizal fungi, can suppress plant diseases through various mechanisms (Vimal *et al*., 2017; Yang *et al*., 2017). These microbes stimulate the production of phytohormones (Kurepin *et al*., 2015) and volatile compounds (Bhattacharyya *et al*., 2015), enhance the transformation and acquisition of nitrogen (Bell *et al*., 2015), mineralize organic phosphorus (Bhattacharyya and Jha, 2012), compete with pathogens for nutrients, and induce systemic resistance to pathogens (Mendes *et al*., 2013). Through these beneficial microbes, the soil maintains a good ecological environment. However, some soil pathogens can propagate excessively and break through this protective shield, giving rise to plant diseases (Mendes *et al*., 2013). Therefore, studies on the composition and diversity of rhizosphere microbiomes are critical in finding methods of improving plant health and productivity.

High-throughput sequencing has been widely used to determine the compositions and diversities of various plant rhizosphere microbiomes, such as *Arabidopsis*, *Populus*, rice, barley, and maize (Gottel *et al*., 2011; Bulgarelli *et al*., 2012; Lundberg *et al*., 2012; Peiffer *et al*., 2013; Schlaeppi *et al*., 2014; Bulgarelli *et al*., 2015; Edwards *et al*., 2015; Walters *et al*., 2018). In *Arabidopsis* roots, Proteobacteria, Actinobacteria, and Bacteroidetes are the dominant bacterial phyla, and root-inhabiting microbiota differ significantly from the microbiota inhabiting the rhizosphere and unplanted soil (Bulgarelli *et al*., 2012). Actinobacteria, Bacteroidetes,

*Corresponding author. E-mail: zhuliu@hainanu.edu.cn.

and Proteobacteria are also the predominant phyla in barley roots. Compared to barley roots, samples collected from barley rhizosphere and bulk soil have been shown to possess higher bacterial richness and diversity (Bulgarelli *et al.*, 2015). Although rhizosphere community composition and diversity have been studied in many plants, few studies have focused on microbial interactions within the rhizosphere, especially in arecanut palms.

Microbial interactions are highly complex and dynamic, and are crucial for the maintenance of homeostasis in microbial communities. Interdependent microbes communicate, co-evolve, exchange genetic information (Braga *et al.*, 2016), and further protect plants from diseases and abiotic stresses (Frey-Klett *et al.*, 2011). For example, the *Moniliophthora roreri* phytopathogen and the *Trichoderma harzianum* endophyte cohabit in cacao plants. *Trichoderma harzianum* produces antifungal secondary metabolites that antagonize *Moniliophthora roreri*, enhancing plant disease resistance (Tata *et al.*, 2015). Co-occurrence networks are commonly generated to analyze microbial interactions. In co-occurrence networks, individual microbes are represented as nodes, and the relationships between microbes, including positive and negative correlations, are represented as edges. Synergistic microbes tend to co-occur across samples and show a positive correlation. In contrast, antagonistic microbes tend to compete for the same niche and are negatively correlated (Weiss *et al.*, 2016). Some methods of computing these correlations have been developed, such as the Pearson correlation coefficient, Spearman correlation coefficient, and SparCC correlation coefficient. In particular, the SparCC correlation coefficient is designed for compositional data and can infer high-accuracy correlations even in the most challenging data sets (Friedman and Alm, 2012).

In this study, rhizosphere microbiomes were compared between healthy and root-rotted arecanut palm plants using high-throughput sequencing. The richness, diversities, and compositions of bacterial and fungal communities in different samples were investigated. Positively and negatively correlated microbial micro-communities were identified using co-occurrence networks. The results suggested that root rot altered the rhizosphere microbiomes of arecanut palm, and that ecological imbalance among beneficial microbes in the soil was associated with root rot. Our study identified beneficial microbes that inhibited root rot in arecanut palm and further unraveled the relationship between the rhizosphere microbiome and root rot.

## MATERIALS AND METHODS

### *Sample collection*

A total of 24 soil samples were collected in Baoting County (18°23′58.59″ N, 109°39′27.47″ E), Hainan Province, China, in March 2018. Twelve samples were collected from the rhizosphere (10–15 cm depth) of healthy arecanut palm plants, and another 12 samples were collected from the rhizosphere of root-rotted arecanut palm plants (Fig. S1, see Supplementary Material for Fig. S1). Three healthy or root-rotted samples were pooled together to obtain a total of eight samples (*i.e.*, four healthy samples and four root-rotted samples). The eight samples were then placed in sterile tubes and were snap frozen in liquid nitrogen before being stored at −80 °C until DNA extraction. Disease severity classification was performed according to the symptoms of the root surfaces. Healthy arecanut palm plants exhibited no obvious spots, while root-rotted palm plants exhibited large brown or black rotted areas.

### *Measurement of soil physicochemical properties*

Ten soil physicochemical factors were measured for each sample, according to previous protocols (Bao, 2000). These factors included total nitrogen (TN), ammonium nitrogen ($NH_4^+$), alkali-hydrolyzed nitrogen (AHN), soil organic matter (SOM), soil organic carbon (SOC), total potassium (TK), available potassium (AK), total phosphorus (TP), available phosphorus (AP), and pH. Total nitrogen was determined by the semi-micro Kjeldahl method, while $NH_4^+$ was determined by indophenol blue colorimetry after potassium chloride extraction. Alkali-hydrolyzed nitrogen was determined by the alkaline hydrolysis diffusion method, and SOM was determined by wet oxidation with potassium dichromate. Soil organic carbon was determined based on the SOM content. Total potassium was determined by flame photometry after sodium hydroxide melting, while AK was determined by flame photometry after ammonium acetate extraction. Total phosphorus was determined by molybdenum blue colorimetry after sodium hydroxide melting, and AP was determined by the 0.5 mol $L^{-1}$ sodium bicarbonate method. Soil pH was determined using a glass electrode meter at a soil-to-water ratio (weight/volume) of 1:2.5.

### *DNA extraction, polymerase chain reaction (PCR) amplification, and sequencing*

Microbial DNA was extracted from each sample using the standard protocol of the PowerSoil DNA isolation kit (MO BIO Laboratories, Inc., USA). DNA quality and quantity were assessed using the 260 nm/280 nm and 260 nm/230 nm ratios. The V3–V4 region of the bacterial 16S rRNA gene was amplified using the 338F forward primer (5′-ACTCCTACGGGAGGCAGCA-3′) and the 806R reverse primer (5′-GGACTACHVGGGTWTCTAAT-3′) (Zhou *et al.*, 2017). The fungal ITS region was amplified using the ITS1 forward primer (5′-CTTGGTCATTTAGAGGAAGTAA-3′) and the ITS2 reverse primer (5′-GCTGCGTTCTTCATCGATGC-3′) (Xiong *et al.*, 2016).

The PCR amplification was performed in a total volume of 50 μL, which contained 10 μL buffer, 0.2 μL Q5 High-Fidelity DNA polymerase, 10 μL high GC enhancer, 1 μL dNTP, 1.5 μL forward primer, 1.5 μL reverse primer, 50 ng genomic DNA, and $ddH_2O$. Thermal cycling conditions were as follows: initial denaturation at 95 °C for 5 min, followed by 15 cycles at 95 °C for 1 min, 50 °C for 1 min, and 72 °C for 1 min, with a final extension at 72 °C for 7 min. The PCR products from the first step were purified using VAHTS DNA clean beads (Vazyme Biotech Co., Ltd. China). A second round of PCR was then performed in a 40 μL reaction volume containing 20 μL 2× Phusion HF MM buffer, 8 μL $ddH_2O$, 1 μL forward primer, 1 μL reverse primer, and 10 μL PCR products from the first step. Thermal cycling conditions were as follows: initial denaturation at 98 °C for 30 s, followed by 10 cycles at 98 °C for 10 s, 65 °C for 30 s, and 72 °C for 30 s, with a final extension at 72 °C for 5 min. Finally, all PCR products were quantified using Quant-iT dsDNA HS reagent, pooled together and paired-end sequenced (2 × 250) on the Illumina HiSeq 2500 platform at Biomarker Technologies Corporation (Beijing, China). Index (barcode) sequences were employed as sample-specific identifiers to distinguish reads from different samples, and the reads were deposited in the NCBI Sequence Read Archive (SRA) under BioProject accession number PRJNA591320.

Reads were overlapped and merged to generate continuous tags using FLASH (Magoč and Salzberg, 2011). The overlap length was at least 10 bp, and the ratio of mismatched base pairs within the overlap was 0.2 at most. The tags were truncated at the start of a 50 bp sliding window using Trimmomatic (Bolger *et al*., 2014) when the average quality within the window was below 20. Truncated tags shorter than 75% of the original length, as well as the chimaeras identified by UCHIME (Edgar *et al*., 2011), were discarded. Tags with at least 97% similarity were clustered into operational taxonomic units (OTUs) using USEARCH (Edgar, 2013). The OTUs with abundances less than 0.005% of the total sequences were further eliminated (Bokulich *et al*., 2013). The taxonomic information for the representative sequence of each OTU was annotated using the Ribosomal Database Project (RDP) classifier (Wang *et al*., 2007) against the SILVA database (Quast *et al*., 2013) and the UNITE database (Kljalg *et al*., 2013) for bacteria and fungi, respectively.

### *Statistical analyses*

Alpha diversity indexes including Chao1 and Shannon, were calculated in Mothur (Schloss *et al*., 2009). Principal coordinate (PCo) analysis (PCoA) based on the Bray-Curtis and UniFrac distances were performed in QIIME (Caporaso *et al*., 2010). Differentially abundant OTUs were identified using the EdgeR generalized linear model (GLM) approach (Edwards *et al*., 2015). Permutational multivariate analysis of variance (PERMANOVA), redundancy analysis (RDA), and the Mantel test were performed using the 'vegan' package in R.

### *Construction of co-occurrence networks*

To build high-confidence co-occurrence networks, low-abundance OTUs with less than 5 counts were eliminated. The SparCC correlation coefficients between the remaining OTUs were calculated for the healthy and root-rotted samples. One-hundred shuffles were performed, and the SparCC correlation coefficients for each of the shuffled data sets were recalculated to generate the $P$ values. Two OTUs were considered correlated if their SparCC correlation coefficient was $\geqslant 0.7$ or $\leqslant -0.7$ and if the $P$ value was 0. The co-occurrence network was constructed using the OTUs that were only correlated in the root-rotted samples but not in the healthy samples. Furthermore, the bacterial co-occurrence network was divided into modules using the Markov cluster algorithm. Each module included at least 5 OTUs.

## RESULTS

### *Soil physicochemical characteristics*

The physicochemical characteristics (TN, $NH_4^+$, AHN, SOM, SOC, CK, AK, TP, AP, and pH) of samples collected from the rhizosphere of healthy and root-rotted arecanut palm plants are shown in Table SI (see Supplementary Material for Table SI). The concentrations of AHN, AK, and AP, as well as the pH values, were significantly higher (Wilcoxon's test, $P < 0.05$) in the root-rotted samples than in the healthy samples. The concentration of TK was significantly lower (Wilcoxon's test, $P < 0.05$) in the root-rotted samples than in the healthy samples, while the levels of TN, $NH_4^+$, SOM, SOC, and TP did not differ significantly between the root-rotted and healthy samples.

### *Alpha and beta diversitiy indexes differ between the healthy and root-rotted samples*

To determine the association between the rhizosphere microbiome and root rot of arecanut palm, the V3–V4 region of the bacterial 16S rRNA gene and the fungal ITS region were sequenced. For the bacterial community, a total of 206 867 and 251 814 reads were detected in the healthy and root-rotted samples, respectively. After filtering low-quality, short, and chimeric sequences, 150 686 and 179 257 sequences were obtained for the healthy and root-rotted samples, respectively. The bacterial sequences were then clustered into 6 344 OTUs (ranging from 1 517 to 1 685) for the healthy samples and 7 211 OTUs (ranging from 1 774 to 1 813) for the root-rotted samples, based

on a 97% similarity level (Table SII, see Supplementary Material for Table SII). For the fungal community, 318 614 and 320 164 reads in the healthy and root-rotted samples, respectively, were assembled to 280 755 and 283 375 high-quality sequences, respectively. Furthermore, 2 810 OTUs (ranging from 636 to 769) for the healthy samples and 3 250 OTUs (ranging from 729 to 866) for the root-rotted samples were obtained (Table SII).

Alpha diversity indexes including Chao1 and Shannon index were used to evaluate microbial richness and diversity, respectively. Compared to the healthy samples, the root-rotted samples had significantly higher (Wilcoxon's test, $P < 0.05$ for bacterial and fungal communities) Chao1 values (Fig. 1a, Fig. S2a, see Supplementary Material for Fig. S2a), *i.e.*, higher bacterial and fungal richness. Notably, bacterial richness was higher in the root-rotted samples than in the healthy samples. According to the Shannon index, bacterial diversity was also significantly higher (Wilcoxon's test, $P < 0.05$) in the root-rotted samples than in the healthy samples (Fig. 1b). However, there was no significant difference in fungal diversity between the healthy and root-rotted samples according to Shannon index (Fig. S2b, see Supplementary Material for Fig. S2b). These results showed that root rot had overall effects on soil microbial richness and diversity.

To further ascertain the differences in microbiota between the healthy and root-rotted samples, beta diversity indexes were analyzed using PCoAs based on Bray-Curtis and UniFrac distances. Bray-Curtis distance is based on the abundance of taxa and can quantify the dissimilarity in the bacterial or fungal communities between different samples. On the other hand, UniFrac distance considers both abundance and phylogenetic relatedness, but it is not suitable for fungal community comparisons. For the bacterial community, in both Bray-Curtis and UniFrac PCoAs, the healthy and root-rotted samples were divided into distinct clusters and were separated across the first principal coordinate (PERMANOVA, $P < 0.05$ based on Bray-Curtis and UniFrac distances) (Fig. 2a, Fig. S3a, see Supplementary Material for Fig. S3a). These results revealed that the healthy and root-rotted samples harbored distinct bacterial microbiomes. Moreover, the bacterial microbiomes from the root-rotted samples had higher heterogeneity (Wilcoxon's test, $P < 0.01$ based on UniFrac distance, and $P < 0.05$ based on Bray-Curtis distance) than those from the healthy

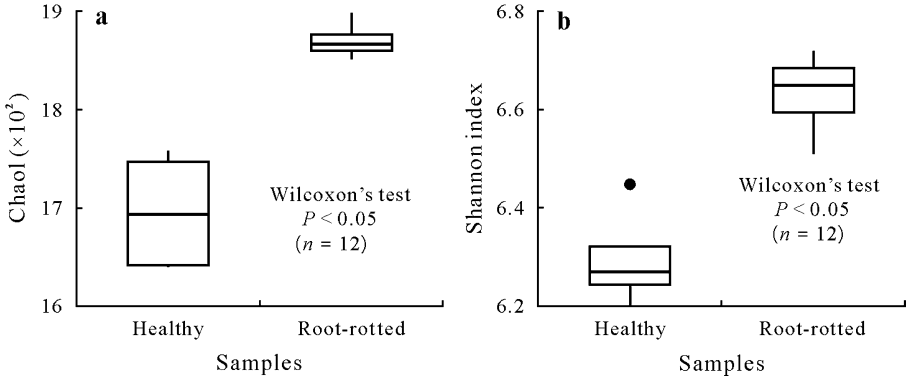


Fig. 1 Comparison of alpha diversity indexes for bacterial community in samples collected from the rhizosphere of healthy and root-rotted arecanut palm plants: Chao1 (a) and Shannon indexes (b). Wilcoxon's test is used to evaluate the difference in Chao1 or Shannon index between the healthy and root-rotted samples. The range of the box is from the first quartile to the third. The black line represents the median. The filled circle represents the outlier.

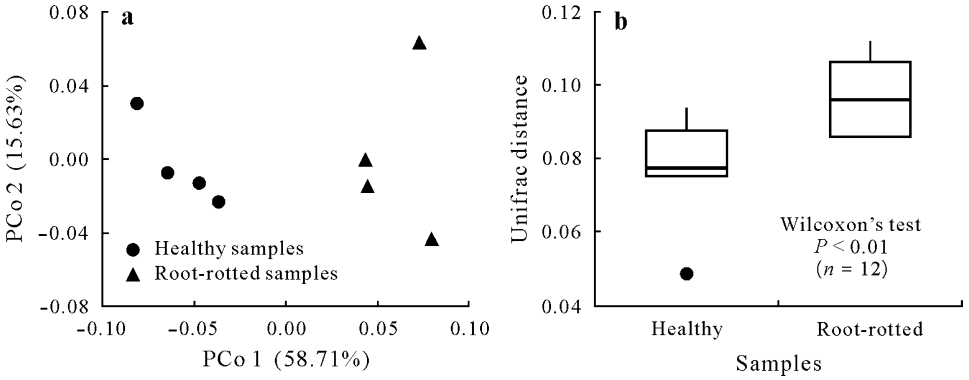


Fig. 2 Bacterial microbiota separation for samples collected from the rhizosphere of healthy and root-rotted arecanut palm plants: principal coordinate (PCo) analysis based on UniFrac distance (a) and UniFrac distance measurement for differences of bacterial community between different samples within each group (b). UniFrac distances are further compared between the healthy and root-rotted samples using Wilcoxon's test. The range of the box is from the first quartile to the third. The black line represents the median. The filled circle represents the outlier.

samples (Fig. 2b, Fig. S3c; see Supplementary Material for Fig. S3c). Similar trends were also observed in the Bray-Curtis PCoA of the fungal community (PERMANOVA, $P < 0.05$) (Fig. S3b, see Supplementary Material for Fig. S3b), except that there was no notable difference in heterogeneity between the healthy and root-rotted samples (Fig. S3d, see Supplementary Material for Fig. S3d).

*Healthy and root-rotted samples exhibit distinct microbial community compositions*

To identify key microbes that accounted for the observed microbiota separation, community composition was analyzed. Proteobacteria, Acidobacteria, Actinobacteria, Chloroflexi, and Bacteroidetes were found to be the five dominant phyla in the root-rotted samples, representing 81.88% of bacterial abundance (Fig. 3a). In the healthy samples, Gemmatimonadetes replaced Bacteroidetes as the fifth dominant phylum (Fig. 3a). Unlike the unclassified bacterial phyla, unclassified fungal phyla had higher relative abundances, representing 20.18% and 25.31% of the overall abundance in the root-rotted and healthy samples, respectively (Fig. S4a, see Supplementary Material for Fig. S4a). Ascomycota and Basidiomycota fungi were predominant in both the root-rotted and healthy samples, with Ascomycota occupying more than half of the total fungal abundance (Fig. S4a).

The relative abundances of various phyla were compared between the healthy and root-rotted samples. Significant differences (Wilcoxon's test, $P < 0.05$) were found in bacterial phyla (Fig. 3b). Compared with the healthy samples, higher relative abundances of Proteobacteria, Bacteroidetes, Saccharibacteria, Parcubacteria, Cyanobacteria, and Fibrobacteres were found in the root-rotted samples, while Acidobacteria, Gemmatimonadetes, and GAL15 were absent. Similarly, fungal phyla also exhibited significant differences (Wilcoxon's test, $P < 0.05$) between the healthy and root-rotted samples (Fig. S4b, see Supplementary Material for Fig. S4b). In the root-rotted samples, higher relative abundances of Chytridiomycota and Mortierellomycota were found, while there was lower relative abundance of Calcarisporiellomycota.

For a more detailed characterization of the microbiomes, differentially abundant OTUs were identified by fitting a GLM. A total of 241 bacterial OTUs and 19 fungal OTUs were significantly enriched, and 159 bacterial OTUs and 33 fungal OTUs were significantly absent ($P < 0.05$) in the root-rotted samples relative to the healthy samples (Fig. 4, Fig. S5, see Supplementary Material for Fig. S5). Most of the enriched bacterial OTUs belonged to the alpha-, beta-, gamma-Proteobacteria, and Sphingobacteriia classes, with the OTUs of gamma-Proteobacteria having the largest fold change (Fig. 4). The OTUs of Sphingobacteriia were mainly categorized into the Chitinophagaceae family, which is associated with chitin degradation (Hargreaves *et al.*, 2015). *Nocardioides* and *Pseudomonas* were the most prominent genera in the root-rotted samples, and some members within *Pseudomonas* are capable of infecting plants (Walker *et al.*, 2004; Xin and He, 2013). The enriched fungal OTUs were categorized as belonging to the Agaricomycetes and Sordariomycetes classes, with the dominant genera being *Mortierella*, *Psathyrella,* and *Paraglomus* in the root-rotted samples.

The absent bacterial OTUs in the root-rotted samples were mainly consisted of Ktedonobacteria, Gemmatimonadetes, and Acidobacteria phyla. Interestingly, the absent fungal OTUs also mainly belonged to Agaricomycetes and

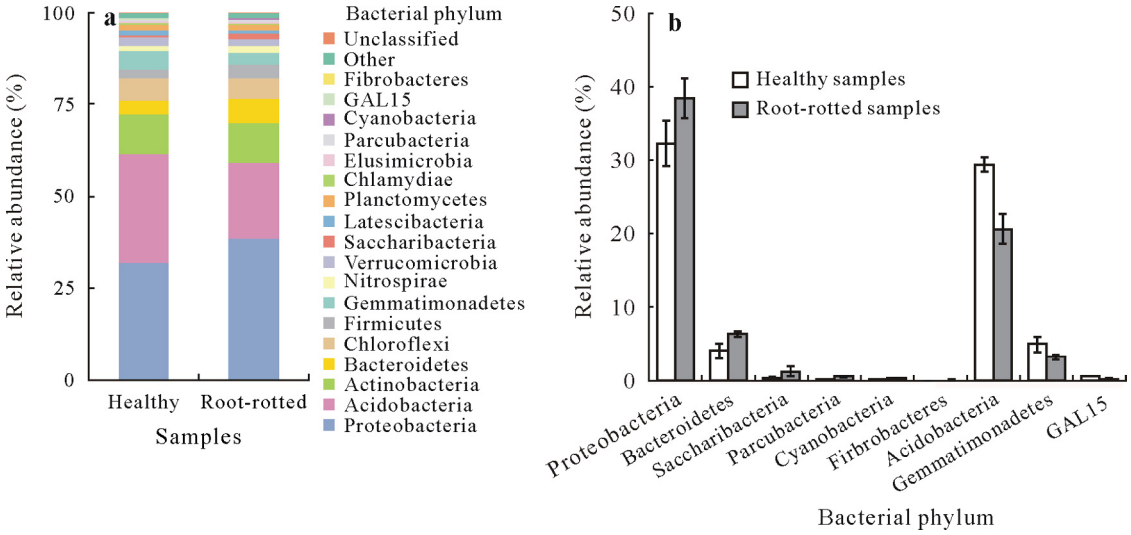


Fig. 3 Comparison of bacterial community composition for samples collected from the rhizosphere of healthy and root-rotted arecanut palm plants: average relative abundances of various bacterial phyla in the healthy and root-rotted samples (a) and bacterial phyla that differed significantly (Wilcoxon's test, $P < 0.05$) between the healthy and root-rotted samples (b). The error bar represents the standard deviation of mean ($n = 12$).

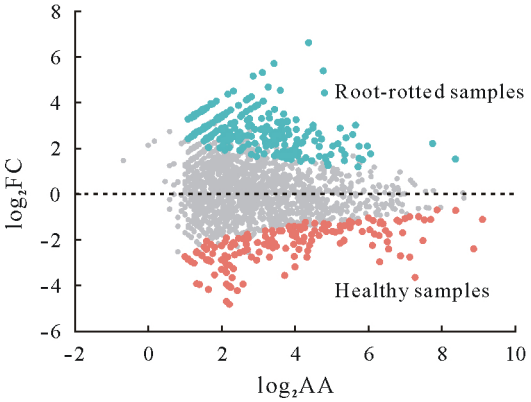


Fig. 4 Differentially abundant operational taxonomic units (OTUs) of bacterial communities in healthy and root-rotted samples collected from the rhizosphere of arecanut palm plants. Each filled circle represents one OTU. For each OTU, the average abundance and the fold change were computed, followed by log transformation. Blue and red filled circles represent 241 and 159 significantly enriched OTUs (generalized linear model, $P < 0.05$) in the root-rotted and healthy samples, respectively. Gray filled circles represent the OTUs that have no significant difference between the root-rotted and healthy samples. FC = fold change; AA = average abundance.

Sordariomycetes classes, which was consistent with the enriched OTUs in the root-rotted samples. This is probably due to the high relative abundances of Ascomycota and Basidiomycota phyla. In addition, 69 bacterial OTUs were attributed to the Bacteroidia and Clostridia classes, and 175 fungal OTUs were mainly derived from Agaricomycetes and Sordariomycetes classes in the root-rotted samples. In contrast, only 3 bacterial OTUs and 3 fungal OTUs were unique to the healthy samples.

*Co-occurrence networks reveal correlated micro-communities*

To identify correlated microbes in the context of root rot, the SparCC correlation coefficients between OTUs were calculated. A total of 505 and 437 pairs of OTUs, which were positively and negatively correlated, constituted the bacterial co-occurrence network. Similarly, 22 and 25 pairs of OTUs, which were positively and negatively correlated, constituted the fungal co-occurrence network. In the bacterial co-occurrence network, the degree of OTU350 belonging to the Acidimicrobiales order was the highest. It had 20 positively correlated OTUs, mainly from the Rhodospirillales and Gaiellales orders, and 9 negatively correlated OTUs from the Solibacterales, Rhizobiales, Nitrosomonadales, and Myxococcales orders. In the fungal co-occurrence network, OTU765 had the highest degree, and its 4 positively correlated OTUs were from the *Hypomyces, Colletotrichum*, and *Cyphellophora* genera. In addition, it had one negatively correlated OTU from the Glomerales order.

The bacterial co-occurrence network was divided into 15 modules based on the Markov cluster algorithm (Fig. 5). OTU83, OTU920, and OTU1701, belonging to the *Acidothermus* genus, were assigned to modules 2, 4, and 11, respectively. OTU37 and OTU30, belonging to the *Bacillus* genus, were assigned to modules 3 and 15, respectively. The fungal co-occurrence network was not an interconnected network, but was instead made up of several subnetworks (Fig. S6, see Supplementary Material for Fig. S6). Similarly, OTU40, OTU220, OTU12, and OTU90, all belonging to the *Penicillium* fungal genus, were also located in different subnetworks. The results showed that bacteria or fungal species from the same genus could respond to different environments.

We focused on the largest module in the bacterial co-occurrence network, *i.e.*, module 1 (Fig. 6a). In module 1, 40 and 15 pairs of OTUs were positively and negatively correlated, respectively. The OTUs generally belonged to the Rhodospirillales, Nitrosomonadales, Acidobacteriales, Gaiellales, and Blastocatellales orders. The number of OTUs from Rhodospirillales was the largest, and they were positively correlated with each other. Moreover, the OTUs from Rhodospirillales were also positively correlated with the OTUs from Acidimicrobiales and Acidobacteriales, but were negatively correlated with the OTUs from Blastocatellales and Myxococcales. The OTUs from the Acidimicrobiales and Acidobacteriales orders were negatively correlated with the OTUs from the Myxococcales and Nitrosomonadales orders. The OTU belonging to Acidobacteriales was also negatively correlated with the OTU belonging to Blastocatellales. As expected, the OTUs from Nitrosomonadales were positively correlated with the OTUs representing Blastocatellales and Myxococcales. In summary, the bacterial species in Rhodospirillales, Acidimicrobiales, and Acidobacteriales constituted a positively-correlated micro-community, and the bacterial species in Blastocatellales, Myxococcales, and Nitrosomonadales established another micro-community (Fig. 6b). The two micro-communities were negatively correlated in the root-rotted samples. However, no such pattern was observed in the fungal co-occurrence network. Instead, fungal species within the same order showed negative correlations; for example, OTU4 and OTU222 from the Hypocreales order.

*Relationships between microbial community and environmental factors*

Environmental changes have an impact on the soil microbial community (Valentin-Vargas *et al.*, 2014; Zhao *et al.*, 2018). To evaluate the effects of AHN, AK, AP, pH, and TK on microbial community structure, RDA was performed. The first and second RDA components explained 45.35% and 14.96% of the bacterial community variation, respectively (Fig. 7). The root-rotted and healthy samples were separated along the first component, as in the PCoAs

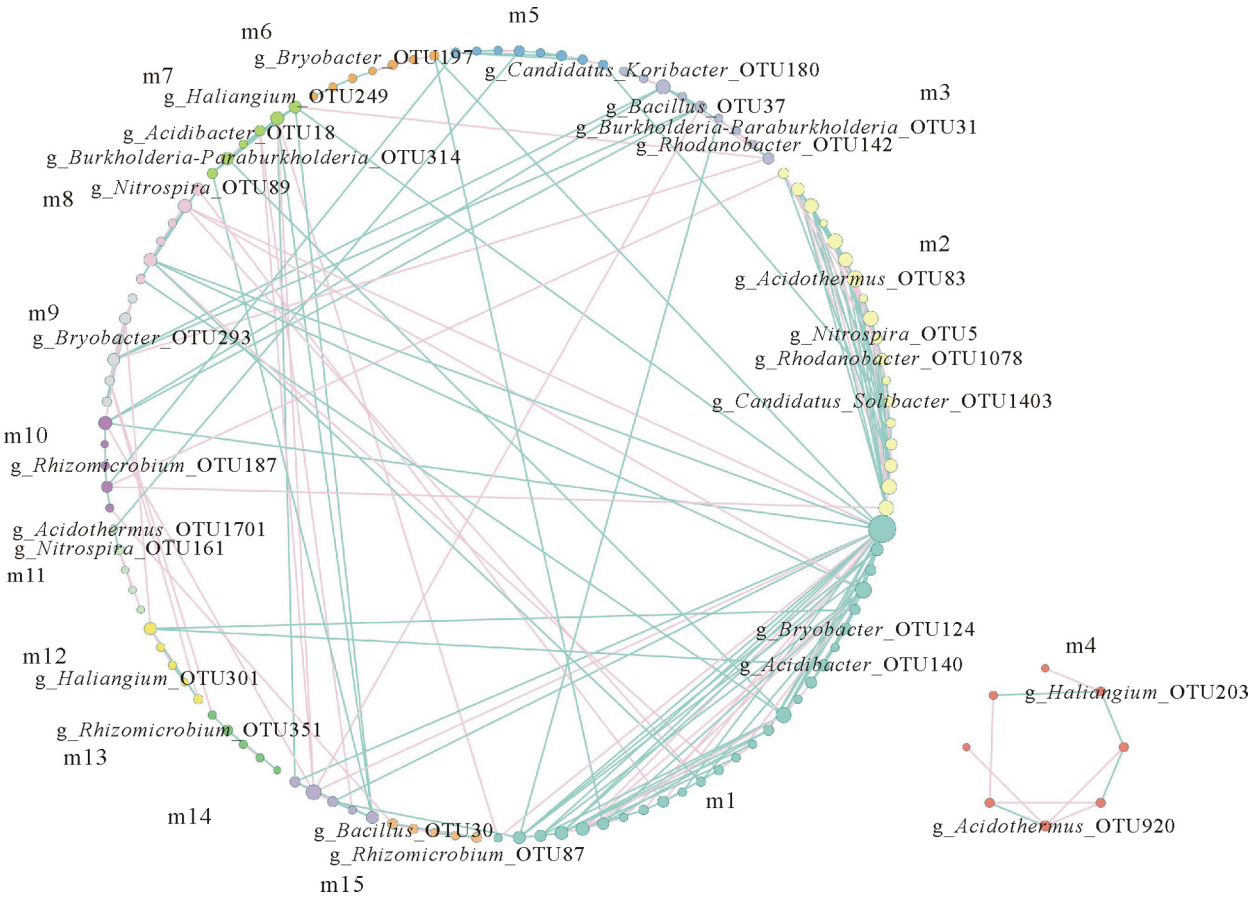


Fig. 5 Bacterial co-occurrence network modules. The bacterial co-occurrence network is divided into 15 modules (m1–m15), and each filled circle represents an operational taxonomic unit (OTU). Green and pink lines represent positively and negatively correlated OTUs, respectively. The OTUs from the same module are marked with the same color. The larger filled circle denotes a higher degree. g = genus.

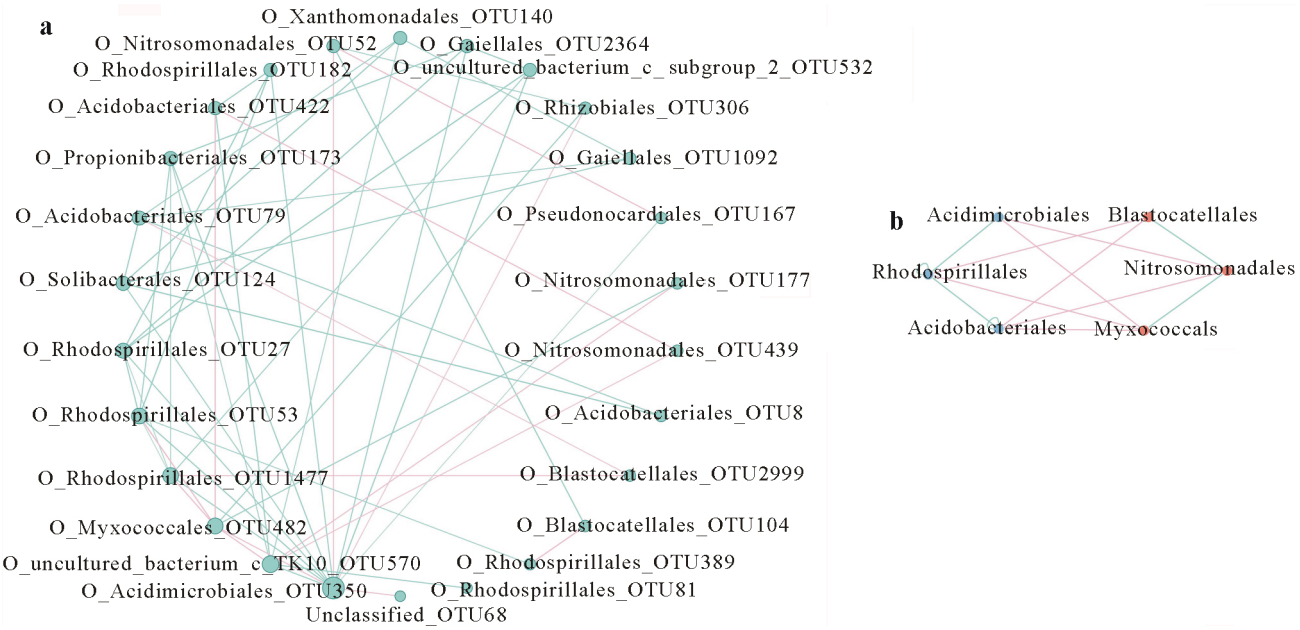


Fig. 6 Correlated operational taxonomic units (OTUs) (a) and orders (b) in the largest module in the bacterial co-occurrence network. Each filled circle represents an OTUs, the larger filled circle denotes a higher degree, and green and pink lines represent positively and negatively correlated OTUs, respectively in a. Blue and red filled circles individually constitute two positively correlated (green lines) micro-communities and there are negative correlations (pink lines) between members of the two micro-communities in b. O = order; c = class.

of the bacterial community. Bacterial community composition was significantly correlated with the five environmental factors according to the Mantel test ($R = 0.67$, $P < 0.05$). Compared to AP, pH, and TK, both AHN ($R = 0.67$, $P < 0.01$) and AK ($R = 0.74$, $P < 0.01$) affected the microbial community more significantly, indicating that AHN and AK were the primary factors that shaped bacterial community composition. For the fungal community, 22.28% and 19.79% of the variation could be explained by the first and second RDA components, respectively (Fig. S7, see Supplementary Material for Fig. S7). The second component clearly distinguished the root-rotted samples from the healthy samples. However, only pH had a significant effect on fungal community variation based on the Mantel test ($R = 0.47$, $P < 0.05$).

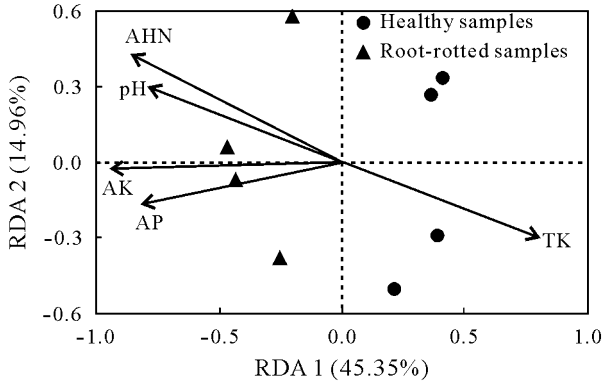


Fig. 7 Redundancy analysis (RDA) of bacterial community in healthy and root-rotted samples collected from the rhizosphere of arecanut palm plants. Arrows indicate the direction and magnitude of how soil physicochemical factors were associated with bacterial community structure. AHN = alkali-hydrolyzed nitrogen; AK = available potassium; AP = available phosphorus; TK = total phosphorus.

## DISCUSSION

Although root rot has greatly hampered arecanut production, to the best of our knowledge, few studies have been conducted on root rot in arecanut palm. Thus, to determine the relationship between root rot and the rhizosphere microbiome, samples were collected from the rhizosphere of healthy and root-rotted arecanut palm plants. Microbial richness and diversities were compared between the root-rotted and healthy samples using Chao1 and Shannon index, which revealed that the root-rotted samples had significantly higher bacterial richness and diversities, as well as higher fungal richness, than the healthy samples. Our results contradict those of previous studies, which have generally reported that the microbial diversity of the rhizosphere is positively associated with plant health (Luan *et al*., 2015). It has also been reported that highly diverse microbial communities increase resistance to pathogen invasions and decrease the chances of disease outbreaks (van Elsas *et al*., 2012; Yang *et al*., 2017). However, some studies have shown that higher microbial diversity is not always beneficial or healthier (Shade, 2017; Reese and Dunn, 2018). For example, the diversity and number of strictly anaerobic bacteria were found to be increased in women with bacterial vaginosis compared to in healthy women (Ma *et al*., 2012).

In the current study, the healthy and root-rotted samples were separated in Bray-Curtis and UniFrac PCoAs, suggesting that these samples harboured distinct microbiomes. To further determine which microbes played an important role in this process, microbial community compositions were compared between the healthy and root-rotted samples. Proteobacteria, Acidobacteria, Actinobacteria, and Chloroflexi were the most dominant bacterial phyla in both the root-rotted and healthy samples, which suggests that root rot did not change the dominant soil phyla, although it did change the proportions of these dominant phyla. The relative abundances of the Proteobacteria, Bacteroidetes, Saccharibacteria, Parcubacteria, Cyanobacteria, and Fibrobacteres phyla were significantly higher in the root-rotted samples than in the healthy samples. Members of Proteobacteria are typically gram-negative bacteria, some of which are plant pathogens, while Bacteroidetes members are opportunistic pathogens that infect various plants by degrading plant cell wall components such as pectin and agar (Thomas *et al*., 2011). Isolating the microbes enriched in the root-rotted samples is an important step in ascertaining the causal agents of root rot. The relative abundances of potentially beneficial bacteria, *i.e.*, Acidobacteria, Gemmatimonadetes, and GAL15, were found to be higher in the healthy samples, which is in accordance with a previous study (Yin *et al*., 2013). Acidobacteria members are able to suppress tobacco black root rot disease (Kyselkov *et al*., 2009), potato common scab (Rosenzweig *et al*., 2012), banana *Fusarium* wilt disease (Shen *et al*., 2015), strawberry *Fusarium* wilt disease (Cha *et al*., 2016), and vanilla *Fusarium* wilt disease (Xiong *et al*., 2017). Similarly, a high relative abundance of Gemmatimonadetes has also been found in strawberry *Fusarium* wilt-suppressive soil (Cha *et al*., 2016). A negative correlation between Gemmatimonadetes and the incidence of banana *Fusarium* wilt disease has also been reported (Shen *et al*., 2014). These results indicated that Acidobacteria and Gemmatimonadetes members may potentially be biocontrol agents against root rot in arecanut palm.

In terms of the fungal community, Ascomycota and Basidiomycota were the predominant phyla, with the relative abundance of Ascomycota exceeding 50% in both the root-rotted and healthy samples. Some Ascomycota members form symbiotic associations with the root systems of plants, which is conducive to plant growth. However, other members cause plant diseases, such as the *Arthrinium* (Wang *et al*., 2018) and *Aspergillus* (van de Veerdonk *et al*., 2017) genera,

which may be the reason for the appearance and high relative abundances of *Arthrinium* and *Aspergillus* in the root-rotted samples. Similarly, Chytridiomycota and Mortierellomycota had significantly higher relative abundances in the root-rotted samples compared to the healthy samples, while the relative abundance of Calcarisporiellomycota was reduced. Members of Chytridiomycota are unique fungi that have motile stages in their life cycles. Some of these fungi, such as Spizellomyces, are plant pathogens (Joneson *et al*., 2011), and Spizellomyces exhibited a higher relative abundance in the root-rotted samples. The *Delfinachytrium* and *Operculomyces* genera belonging to Chytridiomycota were only found in the root-rotted samples, suggesting that they may be root rot pathogens in arecanut palm. In addition, the relative abundance of the *Mortierella* genus was significantly higher in the root-rotted samples, which may be explained by the fact that *Mortierella* is resistant to several fungicides, allowing the fungus to survive in fumigated soil and re-colonize (Hu *et al*., 2014).

To establish the relationship between microbes and root rot, only OTU pairs that were correlated in the root-rotted samples were selected, after which bacterial and fungal co-occurrence networks were constructed. It was observed that the positively correlated OTUs tended to co-occur in a synergistic manner. On the contrary, the negatively correlated OTUs were inclined to compete and were antagonistic in nature. In the bacterial co-occurrence network, a total of 505 and 437 pairs of OTUs were positively and negatively correlated, respectively. While in the fungal co-occurrence network, only 22 and 25 pairs of OTUs were positively and negatively correlated, respectively. The number of correlated OTUs in the fungal co-occurrence network was far less than that in the bacterial co-occurrence network, indicating that fungal species were inclined to grow independently.

The degree of a particular node in the network represents the number of edges connecting other nodes. A node with a higher degree means that the node has more important functions. In the bacterial co-occurrence network, OTU350 had the highest degree, which suggested that it played a vital role in the bacterial community. However, OTU350 could only be annotated at the order level, *i.e*., Acidimicrobiales. A total of nine OTUs from the Solibacterales, Rhizobiales, Nitrosomonadales, and Myxococcales orders were negatively correlated with OTU350. It has been reported that these four orders participate in the nitrogen cycle (Wang *et al*., 2016; Tu *et al*., 2017). Therefore, Acidimicrobiales members might compete with those from these four orders for some substances in the nitrogen cycle. In the fungal co-occurrence network, OTU765 had the highest degree, but its taxonomic information was incomplete, as only one phylum was known, *i.e.*, Ascomycota. It was, however, interesting that the OTUs that were positively correlated with OTU765 were mainly assigned to plant pathogens, *i.e*., the *Hypomyces*, *Colletotrichum*, and *Cyphellophora* genera. Notably, members of *Colletotrichum* are common plant anthracnose pathogens (Diao *et al*., 2017). The OTU that was negatively correlated with OTU765 was from the Glomerales order, which is involved in the control of rhizosphere pathogens. Furthermore, two negatively correlated micro-communities were identified in the bacterial co-occurrence network. One micro-community consisted of Rhodospirillales, Acidimicrobiales, and Acidobacteriales, while the other included Blastocatellales, Myxococcales, and Nitrosomonadales. Almost all of these six bacterial orders are conducive to plant growth, which implies that ecological imbalance among beneficial bacteria may provide opportunities for pathogens to cause root rot in arecanut palm.

The physicochemical factors AK, pH, and AP are important indicators of soil fertility (Bogunovic *et al*., 2017). In the current study, concentrations of AP, TK, AHN, and AK, as well as pH values, were differed significantly between the root-rotted and healthy samples, and these five factors shaped microbial community composition. The results implied that it may be possible to mitigate root rot by improving soil properties *via* agronomic practices. In particular, pH affected not only the bacterial but also the fungal community, and this result could partly be due to the narrow pH range tolerated by most microbes (Xue *et al*., 2017). In fact, each type of microbe has an optimal pH, and a slight variation may result in ecological imbalance. In addition, pH may impact other soil physicochemical characteristics and indirectly affect the microbial community structure. The pH was higher in the root-rotted samples, which is in accordance with the negative correlation between pH and the ability of soil to suppress pathogens (Svenningsen *et al*., 2018). It was observed that higher pH values increased the relative abundances of pathogenic bacteria such as Bacteroidetes and decreased the relative abundances of beneficial bacteria such as Acidobacteria. These results are also in accordance with previous studies (Rosenblum *et al*., 2009; Xue *et al*., 2017). Collectively, we propose that under normal conditions, plant roots, soil, and rhizosphere microbes maintain a dynamic ecological balance. However, under unfavorable soil physicochemical conditions resulting from continuous cropping and/or unnecessary fertilization, the microbial community structure is altered, thereby gradually allowing potential pathogens to become the dominant population, hence causing plant disease.

## CONCLUSIONS

The current study revealed that the richness, diversity, and composition of the microbial community differed in root-rotted arecanut palm rhizosphere samples compared to in healthy arecanut palm samples. The relative abundances of potential plant pathogens such as Proteobacteria, Bacteroidetes, Chytridiomycota, and Mortierellomycota were

higher in the root-rotted samples, while there was a decrease in potential beneficial bacteria such as Acidobacteria and Gemmatimonadetes. Based on the bacterial co-occurrence network, an ecological imbalance among beneficial bacteria was observed in the root-rotted samples. Furthermore, the Mantel test revealed that pH played an important role in shaping the microbial community composition. Higher pH values tended to reduce the suppressive effects of the soil on arecanut palm root rot by decreasing the abundances of beneficial bacteria and by increasing the abundances of harmful bacteria. The results of this study, therefore, deepen our understanding of the association between the microbial community and root rot in arecanut plant.

## ACKNOWLEDGEMENTS

This work was supported by the Hainan Major Research Project for Science and Technology, China (No. zdkj201817). This work was partly supported by the National Transgenic Major Project of China (No. 2019ZX08010-004), the National Natural Science Foundation of China (Nos. 31560021, 31772887, and 31860676), the Hainan Natural Science Foundation, China (No. 319QN161), and the Priming Scientific Research Foundation of Hainan University, China (No. KYQD(ZR)1929). We thank Dr. Jude Juventus Aweya of Shantou University, China and American Journal Experts (AJE) for English language editing.

## SUPPLEMENTARY MATERIAL

Supplementary material for this article can be found in the online version.

## REFERENCES

Bao S D. 2000. Soil Agrochemical Analysis (in Chinese). 3rd Edn. China Agricultural Press, Beijing.

Bell C W, Asao S, Calderon F, Wolk B, Wallenstein M D. 2015. Plant nitrogen uptake drives rhizosphere bacterial community assembly during plant growth. *Soil Biol Biochem*. **85**: 170–182.

Bhattacharyya D, Yu S M, Lee Y H. 2015. Volatile compounds from *Alcaligenes faecalis* JBCS1294 confer salt tolerance in *Arabidopsis thaliana* through the auxin and gibberellin pathways and differential modulation of gene expression in root and shoot tissues. *Plant Growth Regul*. **75**: 297–306.

Bhattacharyya P N, Jha D K. 2012. Plant growth-promoting rhizobacteria (PGPR): Emergence in agriculture. *World J Microbiol Biotechnol*. **28**: 1327–1350.

Bogunovic I, Pereira P, Brevik E C. 2017. Spatial distribution of soil chemical properties in an organic farm in Croatia. *Sci Total Environ*. **584-585**: 535–545.

Bokulich N A, Subramanian S, Faith J J, Gevers D, Gordon J I, Knight R, Mills D A, Caporaso J G. 2013. Quality-filtering vastly improves diversity estimates from Illumina amplicon sequencing. *Nat Methods*. **10**: 57–59.

Bolger A M, Lohse M, Usadel B. 2014. Trimmomatic: A flexible trimmer for Illumina sequence data. *Bioinformatics*. **30**: 2114–2120.

Braga R M, Dourado M N, Araújo W L. 2016. Microbial interactions: Ecology in a molecular perspective. *Braz J Microbiol*. **47**: 86–98.

Bulgarelli D, Garrido-Oter R, Münch P C, Weiman A, Dröge J, Pan Y, McHardy A C, Schulze-Lefert P. 2015. Structure and function of the bacterial root microbiota in wild and domesticated barley. *Cell Host Microbe*. **17**: 392–403.

Bulgarelli D, Rott M, Schlaeppi K, Ver Loren van Themaat E, Ahmadinejad N, Assenza F, Rauf P, Huettel B, Reinhardt R, Schmelzer E, Peplies J, Gloeckner F O, Amann R, Eickhorst T, Schulze-Lefert P. 2012. Revealing structure and assembly cues for *Arabidopsis* root-inhabiting bacterial microbiota. *Nature*. **488**: 91–95.

Caporaso J G, Kuczynski J, Stombaugh J, Bittinger K, Bushman F D, Costello E K, Fierer N, Peña A G, Goodrich J K, Gordon J I, Huttley G A, Kelley S T, Knights D, Koenig J E, Ley R E, Lozupone C A, McDonald D, Muegge B D, Pirrung M, Reeder J, Sevinsky J R, Turnbaugh P J, Walters W A, Widmann J, Yatsunenko T, Zaneveld J, Knight R. 2010. QIIME allows analysis of high-throughput community sequencing data. *Nat Methods*. **7**: 335–336.

Cha J Y, Han S, Hong H J, Cho H, Kim D, Kwon Y, Kwon S K, Crüsemann M, Bok L Y, Kim J F, Giaever G, Nislow C, Moore B S, Thomashow L S, Weller D M, Kwak Y S. 2016. Microbial and biochemical basis of a *Fusarium* wilt-suppressive soil. *ISME J*. **10**: 119–129.

Diao Y Z, Zhang C, Liu F, Wang W Z, Liu L, Cai L, Liu X L. 2017. *Colletotrichum* species causing anthracnose disease of chili in China. *Persoonia*. **38**: 20–37.

Edgar R C, Haas B J, Clemente J C, Quince C, Knight R. 2011. UCHIME improves sensitivity and speed of chimera detection. *Bioinformatics*. **27**: 2194–2200.

Edgar R C. 2013. UPARSE: Highly accurate OTU sequences from microbial amplicon reads. *Nat Methods*. **10**: 996–998.

Edwards J, Johnson C, Santos-Medellín C, Lurie E, Podishetty N K, Bhatnagar S, Eisen J A, Sundaresan V. 2015. Structure, variation, and assembly of the root-associated microbiomes of rice. *Proc Natl Acad Sci USA*. **112**: E911–E920.

Frey-Klett P, Burlinson P, Deveau A, Barret M, Tarkka M, Sarniguet A. 2011. Bacterial-fungal interactions: Hyphens between agricultural, clinical, environmental, and food microbiologists. *Microbiol Mol Biol Rev*. **75**: 583–609.

Friedman J, Alm E J. 2012. Inferring correlation networks from genomic survey data. *PLOS Comput Biol*. **8**: e1002687.

Gottel N R, Castro H F, Kerley M, Yang Z M, Pelletier D A, Podar M, Karpinets T, Uberbacher E, Tuskan G A, Vilgalys R, Doktycz M J, Schadt C W. 2011. Distinct microbial communities within the endosphere and rhizosphere of *Populus deltoides* roots across contrasting soil types. *Appl Environ Microbiol*. **77**: 5934–5944.

Hargreaves S K, Williams R J, Hofmockel K S. 2015. Environmental filtering of microbial communities in agricultural soil shifts with crop growth. *PLOS ONE*. **10**: e0134345.

Hu P, Hollister E B, Somenahally A C, Hons F M, Gentry T J. 2014. Soil bacterial and fungal communities respond differently to various isothiocyanates added for biofumigation. *Front Microbiol*. **5**: 729.

Joneson S, Stajich J E, Shiu S H, Rosenblum E B. 2011. Genomic transition to pathogenicity in chytrid fungi. *PLOS Pathog*. **7**: e1002338.

Kõljalg U, Nilsson R H, Abarenkov K, Tedersoo L, Taylor A F S, Bahram M, Bates S T, Bruns T D, Bengtsson-Palme J, Callaghan T M, Douglas B, Drenkhan T, Eberhardt U, Dueñas M, Grebenc T, Griffith G W, Hartmann M, Kirk P M, Kohout P, Larsson E, Lindahl B D, Lücking R, Martín M P, Matheny P B, Nguyen N H, Niskanen T, Oja J, Peay K G, Peintner U, Peterson M, Põldmaa K, Saag L, Saar I, Schüßler A, Scott J A, Senés C, Smith M E, Suija A, Taylor D L, Telleria M T, Weiss M, Larsson K H. 2013. Towards a unified paradigm for sequence-based identification of fungi. *Mol Ecol*. **22**: 5271–5277.

Kurepin L V, Park J M, Lazarovits G, Bernards M A. 2015. *Burkholderia phytofirmans*-induced shoot and root growth promotion is associated with endogenous changes in plant growth hormone levels. *Plant Growth Regul*. **75**: 199–207.

Kyselková M, Kopecký J, Frapolli M, Défago G, Ságová-Marečková M, Grundmann G L, Moënne-Loccoz Y. 2009. Comparison of rhizobacterial community composition in soil suppressive or conducive to tobacco black root rot disease. *ISME J*. **3**: 1127–1138.

Luan F G, Zhang L L, Lou Y Y, Wang L, Liu Y N, Zhang H Y. 2015. Analysis of microbial diversity and niche in rhizosphere soil of healthy and diseased cotton at the flowering stage in southern Xinjiang. *Genet Mol Res*. **14**: 1602–1611.

Lundberg D S, Lebeis S L, Paredes S H, Yourstone S, Gehring J, Malfatti S, Tremblay J, Engelbrektson A, Kunin V, del Rio T G, Edgar R C, Eickhorst T, Ley R E, Hugenholtz P, Tringe S G, Dangl J L. 2012. Defining the core *Arabidopsis thaliana* root microbiome. *Nature*. **488**: 86–90.

Ma B, Forney L J, Ravel J. 2012. Vaginal microbiome: Rethinking health and disease. *Annu Rev Microbiol*. **66**: 371–389.

Magoč T, Salzberg S L. 2011. FLASH: Fast length adjustment of short reads to improve genome assemblies. *Bioinformatics*. **27**: 2957–2963.

Mendes R, Garbeva P, Raaijmakers J M. 2013. The rhizosphere microbiome: Significance of plant beneficial, plant pathogenic, and human pathogenic microorganisms. *FEMS Microbiol Rev*. **37**: 634–663.

Peiffer J A, Spor A, Koren O, Jin Z, Tringe S G, Dangl J L, Buckler E S, Ley R E. 2013. Diversity and heritability of the maize rhizosphere microbiome under field conditions. *Proc Natl Acad Sci USA*. **110**: 6548–6553.

Peng W, Liu Y J, Wu N, Sun T, He X Y, Gao Y X, Wu C J. 2015. *Areca catechu* L. (Arecaceae): A review of its traditional uses, botany, phytochemistry, pharmacology and toxicology. *J Ethnopharmacol*. **164**: 340–356.

Quast C, Pruesse E, Yilmaz P, Gerken J, Schweer T, Yarza P, Peplies J, Glöckner F O. 2013. The SILVA ribosomal RNA gene database project: Improved data processing and web-based tools. *Nucleic Acids Res*. **41**: D590–D596.

Reese A T, Dunn R R. 2018. Drivers of microbiome biodiversity: A review of general rules, feces, and ignorance. *mBio*. **9**: e01294-18.

Rosenblum J M, Zhang Q W, Siu G, Collins T L, Sullivan T, Dairaghi D J, Medina J C, Fairchild R L. 2009. CXCR3 antagonism impairs the development of donor-reactive, IFN-gamma-producing effectors and prolongs allograft survival. *Transplantation*. **87**: 360–369.

Rosenzweig N, Tiedje J M, Quensen III J F, Meng Q X, Hao J J. 2012. Microbial communities associated with potato common scab-suppressive soil determined by pyrosequencing analyses. *Plant Dis*. **96**: 718–725.

Schlaeppi K, Dombrowski N, Oter R G, Ver Loren van Themaat E, Schulze-Lefert P. 2014. Quantitative divergence of the bacterial root microbiota in *Arabidopsis thaliana* relatives. *Proc Natl Acad Sci USA*. **111**: 585–592.

Schloss P D, Westcott S L, Ryabin T, Hall J R, Hartmann M, Hollister E B, Lesniewski R A, Oakley B B, Parks D H, Robinson C J, Sahl J W, Stres B, Thallinger G G, Van Horn David J, Weber C F. 2009. Introducing mothur: Open-source, platform-independent, community-supported software for describing and comparing microbial communities. *Appl Environ Microbiol*. **75**: 7537–7541.

Shade A. 2017. Diversity is the question, not the answer. *ISME J*. **11**: 1–6.

Shen Z Z, Ruan Y Z, Chao X, Zhang J, Li R, Shen Q R. 2015. Rhizosphere microbial community manipulated by 2 years of consecutive biofertilizer application associated with banana *Fusarium* wilt disease suppression. *Biol Fert Soils*. **51**: 553–562.

Shen Z Z, Wang D S, Ruan Y Z, Xue C, Zhang J, Li R, Shen Q R. 2014. Deep 16S rRNA pyrosequencing reveals a bacterial community associated with banana *Fusarium* wilt disease suppression induced by bio-organic fertilizer application. *PLOS ONE*. **9**: e98420.

Svenningsen N B, Watts-Williams S J, Joner E J, Battini F, Efthymiou A, Cruz-Paredes C, Nybroe O, Jakobsen I. 2018. Suppression of the activity of arbuscular mycorrhizal fungi by the soil microbiota. *ISME J*. **12**: 1296–1307.

Tata A, Perez C, Campos M L, Bayfield M A, Eberlin M N, Ifa D R. 2015. Imprint desorption electrospray ionization mass spectrometry imaging for monitoring secondary metabolites production during antagonistic interaction of fungi. *Anal Chem*. **87**: 12298–12305.

Thomas F, Hehemann J H, Rebuffet E, Czjzek M, Michel G. 2011. Environmental and gut *bacteroidetes*: The food connection. *Front Microbiol*. **2**: 93.

Tu Q C, He Z L, Wu L Y, Xue K, Xie G, Chain P, Reich P B, Hobbie S E, Zhou J Z. 2017. Metagenomic reconstruction of nitrogen cycling pathways in a $CO_2$-enriched grassland ecosystem. *Soil Biol Biochem*. **106**: 99–108.

Valentin-Vargas A, Root R A, Neilson J W, Chorover J, Maier R M. 2014. Environmental factors influencing the structural dynamics of soil microbial communities during assisted phytostabilization of acid-generating mine tailings: A mesocosm experiment. *Sci Total Environ*. **500-501**: 314–324.

van de Veerdonk F L, Gresnigt M S, Romani L, Netea M G, Latgé J P. 2017. *Aspergillus fumigatus* morphology and dynamic host interactions. *Nat Rev Microbiol*. **15**: 661–674.

van Elsas J D, Chiurazzi M, Mallon C A, Elhottovā D, Krištůfek V, Salles J F. 2012. Microbial diversity determines the invasion of soil by a bacterial pathogen. *Proc Natl Acad Sci USA*. **109**: 1159–1164.

Vimal S R, Singh J S, Arora N K, Singh S. 2017. Soil-plant-microbe interactions in stressed agriculture management: A review. *Pedosphere*. **27**: 177–192.

Walker T S, Bais H P, Déziel E, Schweizer H P, Rahme L G, Fall R, Vivanco J M. 2004. Pseudomonas aeruginosa-plant root interactions. Pathogenicity, biofilm formation, and root exudation. *Plant Physiol*. **134**: 320–331.

Walters W A, Jin Z, Youngblut N, Wallace J G, Sutter J, Zhang W, González-Peña A, Peiffer J, Koren O, Shi Q J, Knight R, del Rio T G, Tringe S G, Buckler E S, Dangl J L, Ley R E. 2018. Large-scale replicated field study of maize rhizosphere identifies heritable microbes. *Proc Natl Acad Sci USA*. **115**: 7368–7373.

Wang M, Tan X M, Liu F, Cai L. 2018. Eight new *Arthrinium* species from China. *MycoKeys*. **2018**: 1–24.

Wang Q, Garrity G M, Tiedje J M, Cole J R. 2007. Naïve Bayesian classifier for rapid assignment of rRNA sequences into the new bacterial taxonomy. *Appl Environ Microbiol*. **73**: 5261–5267.

Wang W H, Wang H, Feng Y Z, Wang L, Xiao X J, Xi Y G, Luo X, Sun R B, Ye X F, Huang Y, Zhang Z G, Cui Z L. 2016. Consistent responses of the microbial community structure to organic farming along the middle and lower reaches of the Yangtze River. *Sci Rep*. **6**: 35046.

Weiss S, Van Treuren W, Lozupone C, Faust K, Friedman J, Deng Y, Xia L C, Xu Z J Z, Ursell L, Alm E J, Birmingham A, Cram J A, Fuhrman J A, Raes J, Sun F Z, Zhou J Z, Knight R. 2016. Correlation detection strategies in microbial data sets vary widely in sensitivity and precision. *ISME J*. **10**: 1669–1681.

Xin X F, He S Y. 2013. *Pseudomonas syringae* pv. tomato DC3000: A model pathogen for probing disease susceptibility and hormone signaling in plants. *Annu Rev Phytopathol*. **51**: 473–498.

Xiong W, Li R, Ren Y, Liu C, Zhao Q Y, Wu H S, Jousset A, Shen Q R. 2017. Distinct roles for soil fungal and bacterial communities associated with the suppression of vanilla *Fusarium* wilt disease. *Soil Biol Biochem*. **107**: 198–207.

Xiong W, Zhao Q Y, Xue C, Xun W B, Zhao J, Wu H S, Li R, Shen Q R. 2016. Comparison of fungal community in black pepper-vanilla and vanilla monoculture systems associated with vanilla *Fusarium* wilt disease. *Front Microbiol*. **7**: 117.

Xue L, Ren H D, Li S, Leng X H, Yao X H. 2017. Soil bacterial community structure and co-occurrence pattern during vegetation restoration in karst rocky desertification area. *Front Microbiol*. **8**: 2377.

Yang H W, Li J, Xiao Y H, Gu Y B, Liu H W, Liang Y L, Liu X D, Hu J, Meng D L, Yin H Q. 2017. An integrated insight into the relationship between soil microbial community and tobacco bacterial wilt disease. *Front Microbiol*. **8**: 2179.

Yin C T, Hulbert S H, Schroeder K L, Mavrodi O, Mavrodi D, Dhingra A, Schillinger W F, Paulitz T C. 2013. Role of bacterial communities in the natural suppression of *Rhizoctonia solani* bare patch disease of wheat (*Triticum aestivum* L.). *Appl Environ Microbiol*. **79**: 7428–7438.

Zhao Z L, Pan Y J, Jiang J W, Gao S, Sun H J, Dong Y, Sun P H, Guan X Y, Zhou Z C. 2018. Unrevealing variation of microbial communities and correlation with environmental variables in a full culture-cycle of *Undaria pinnatifida*. *Mar Environ Res*. **139**: 46–56.

Zhou Y J, Li J H, Ross Friedman C, Wang H F. 2017. Variation of soil bacterial communities in a chronosequence of rubber tree (*Hevea brasiliensis*) plantations. *Front Plant Sci*. **8**: 849.